

Measurement of Fission Cross-Sections with Lead Slowing-down Spectrometer using Digital Signal Processing

Wataru TAKAHASHI, Takuji OISHI, Mohammad NAKHOSTIN, Takeshi YAMAUCHI
Mamoru BABA, Junichi HORI*, Hideyuki YUKI**, Tsutomu OHTSUKI**

Cyclotron and Radioisotope Center (CYRIC), Tohoku University

Aoba6-3, Aramaki, Aoba-ku, Sendai-shi, Miyagi-ken, 980-8578, Japan

**Research Reactor Institute (KURRI), Kyoto University*

Asasironishi2, Kumatori-cho, Sennan-gun, Osaka-fu, 590-0494, Japan

***Laboratory of Nuclear Science (LNS), Tohoku University*

Mikamine1-2-1, Taihaku-ku, Sendai-shi, Miyagi-ken, 982-0826, Japan

Email: wataru@cyric.tohoku.ac.jp

The energy range of fission cross-section measurement with the lead slowing-down spectrometer at KURRI was extended to about 1 MeV by reducing the electromagnetic noise with a digital signal processing (DSP) technique. We report the results of measurement of neutron induced fission cross-sections of ^{237}Np and ^{241}Am .

1. Introduction

For effective transmutation of minor actinide (MA) in nuclear waste and generation of electricity by Accelerator Driven Systems (ADS), a variety kind of nuclear data are needed. The nuclear data are essential for calculation of reactor characteristics such as critical safety, kinetics, decay heat and so on. Especially, neutron induced fission cross-sections are crucial because the transmutation of the nuclear waste is based on a fission reaction [1].

However, the nuclear data of MA are not enough in quality and quantity. For example, evaluated neutron induced fission cross-sections of ^{237}Np show marked discrepancies each other. Therefore, new measurement is required to improve the data status [2, 3].

A lead slowing-down spectrometer has been used very effectively for measurement of neutron induced fission cross-sections of MA [1-3]. However, the energy range of the measurement was limited below ~10 keV because accelerator-correlated electromagnetic noise piled up on high-energy events. Therefore, we tried and succeeded to extend the energy range of measurement to about 1 MeV by the reduction of the electromagnetic noise with a digital signal processing (DSP) technique [4].

The present study aims to measure neutron induced fission cross-sections of ^{237}Np and ^{241}Am using DSP and to contribute the improvement of these nuclear data. These nuclei account for the greater part of the nuclear waste.

2. Lead slowing-down spectrometer

2.1. The principle and properties of a lead slowing-down spectrometer

The lead isotopes are characterized by a very small capture cross-section, and lead behaves as a non-absorptive substance. Besides, elastic scattering is essentially isotropic and kinetic energy loss is ~1 % per collision. The neutron mean free path is about 2.8 cm. Under these conditions, neutrons slow-down very progressively spreading in space. As a result there is a statistical correlation between slowing-down time t and the mean kinetic energy E that can be expressed as

$$E = \frac{K}{(t + t_0)^2} \dots (*)$$

The value of K is bound to the neutronic properties of lead whereas t_0 is related to the initial kinetic energy of the neutrons [5].

The lead slowing-down spectrometer is very effective for the measurement of small amount of samples with low cross-sections and that of radioactive materials with a high background level, because the neutron intensity is as high as more than thousands times than those in conventional neutron time-of-flight (TOF) method owing to short distance from the source [6]. However the energy resolution of lead slowing-down spectrometer is about 40 % and is lower than those in the TOF method [6].

2.2. Kyoto university lead slowing-down spectrometer

The present measurement was performed using Kyoto University lead slowing-down spectrometer driven by an electron linac (KULS) at KURRI. KULS is a cube of $1.5 \times 1.5 \times 1.5 \text{ m}^3$ and composed of lead blocks ($10 \times 10 \times 20 \text{ cm}^3$, and purity: 99.9%) and set on a steel platform cart in the linac target room. All surfaces of KULS are covered with cadmium sheets of 0.5 mm thick to shield from low energy neutrons. The cross sectional view of KULS is shown in Fig.1 [6].

At the center of KULS, pulsed fast neutrons are produced by a photoneutron target of tantalum (8 cm in diameter and 6 cm in effective thickness) in cylindrical titanium case, which is air-cooled with compressed air [6].

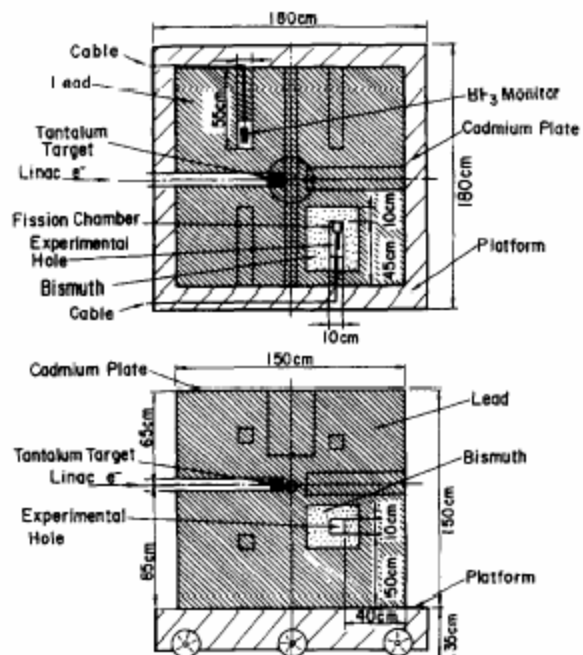


Fig.1 The cross sectional view of KULS [5]

There are eight experimental holes ($10 \times 10 \text{ cm}^2$, 55 or 45 cm in depth) in KULS. The experiment was carried out in one of the experimental holes, which was covered with bismuth layers of 10 to 15 cm in thickness to reduce high energy γ -rays (6 to 7 MeV) produced by the $\text{Pb}(n,\gamma)$ reaction in KULS. Accordingly, the background by the photo-fission events could be ignored in this measurement because the energy of the prompt γ -rays produced by the $\text{Bi}(n,\gamma)$ reaction are lower than the threshold energy for photo-fission reaction [1].

2.3. Energy Calibration of KULS

The energy calibration of KULS was done by using two types of detectors; one was a BF_3 counter for the neutron transmission measurement through a resonance filter that is indium or cobalt, and the other was an Ar gas counter for the capture γ -ray measurement with a resonance filter of gold, copper or aluminum.

The present result for calibration, E vs. t is shown Fig.2. The slowing-down constant K is $193 \pm 2 \text{ (keV} \cdot \mu\text{s}^2)$ and the initial energy constant t_0 is $0.3 \mu\text{s}$. The present values of K and t_0 are in agreement with those reported by Kobayashi et al. [6] However it is probable that the correlation (*) between t and E dose not stand above 100 keV because the inelastic scattering occurs above 0.57 MeV [5]. Therefore now we are promoting calculation for t vs. E , by use of a Monte Carlo code MCNP.

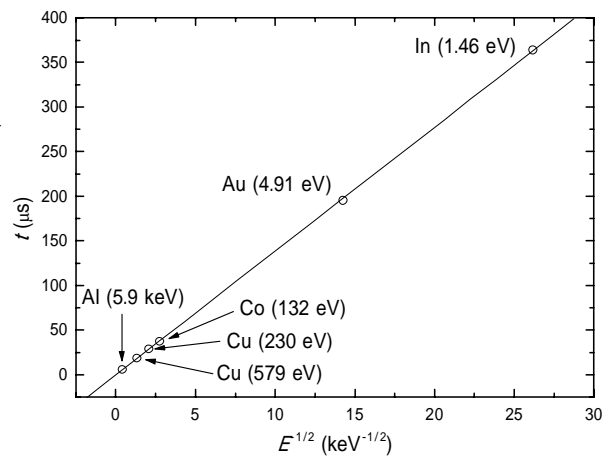


Fig.2 The relation between t and E

2.4. Back-to-back fission chamber

An ionization chamber with two parallel plate electrodes was employed for the detection of fission events. The chamber is made of aluminum, 2 mm thick, and is 40 mm in diameter and 43 mm in length as seen in Fig.3. Since the backsides of MA and ^{235}U deposits face each other, the chamber is called a back-to-back (BTB) type double fission chamber. The distance between the electrode and the deposit layer is 8 mm. The electrodes act as anodes at 300 V from which the fission fragment

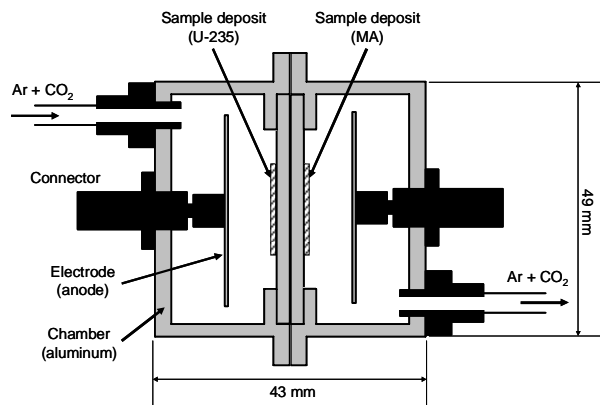


Fig.3 The figure of the BTB chamber

pulses are taken. An Ar + CO₂ gas is flowed through the BTB chamber. The number of atoms for sample deposits was determined through low-geometry α -counting as shown in Table 1.

The signal from the chamber was input into charge-sensitive preamplifier (ORTEC 142PC) , then shaped with a spectroscopy amplifier. The chamber, preamplifier and the cables between the chamber and the preamplifier were heavily wrapped with aluminum foils reduction of electromagnetic noise.

Table 1 The number of atoms for sample deposits

Material	The number of atoms
²³⁵ U (10 μ g)	$(2.80 \pm 0.10) \times 10^{16}$ [7]
²³⁷ Np	$(1.99 \pm 0.02) \times 10^{17}$ [8]
²³⁵ U (5 μ g)	$(1.51 \pm 0.03) \times 10^{16}$ [9]
²⁴¹ Am	$(1.73 \pm 0.02) \times 10^{16}$ [1]

3. Experimental procedure

The pulse width of electron beam was generally 33 ns in FWHM and the frequency was 100 Hz as the optimum value for KULS [5]. The beam current on the target was around 10.5 to 12.4 μ A. The waveform data of the fission fragment pulses were taken from the linear amplifier and digitized and recorded by a digital storage oscilloscope (DSO), LeCroy.

4. Data analysis

Data analysis was performed with the DSP method. The pulse height data and the slowing-down time data were acquired by processing the waveform data. The fission fragment pulses were discriminated from the α -particles pulses by the pulse height [4].

The electromagnetic noise in high-energy region was almost independent of time. Therefore subtraction of the typical waveform data of electromagnetic noise from that of fission fragments enabled great reduction of the electromagnetic noise and extension of the neutron energy range to higher energy. As a result, we could extend the energy range of measurement to about 1 MeV [4].

5. Results and discussion

The present results for neutron induced fission cross-sections of ²³⁷Np and ²⁴¹Am are shown in Fig.4 and Fig.5, respectively. The reference cross-section data of ²³⁵U was taken from JENDL-3.3. The present data are compared with the evaluated nuclear data in JENDL-3.3, ENDF/B- and JEFF-3.1 and other experimental data. The evaluated data are broadened by

40 % in the energy resolution of the KULS to compare with the experimental data.

About the result of ^{237}Np , the present data below 1 keV are in good agreement with the data by Yamanaka et al. [7] and JENDL-3.3. JENDL-3.3 and other experimental data between 1 and 100 keV are 5-30% larger than the present data. The present data above 100 keV differ from JENDL-3.3 markedly probably because the experimental energy resolution becomes gradually worse and the inelastic scattering in lead occurs [8, 10]. For the data in this region, further analysis is needed considering the problem of correlation between t and E .

About the result of ^{241}Am , the present data below 10 keV are in good agreement with JEFF-3.1, but JENDL-3.3, ENDF/B- and other experimental data are smaller than the present data by 5-20 %. The data above 10 keV are 20-80% larger than the evaluated nuclear data probably due to the same reason for ^{237}Np .

References

- [1] T. Kai et al., *Annals of Nuclear Energy*, 28, 723-739 (2001)
- [2] K. Kobayashi et al., *Journal of Nuclear Science and Technology*, 36, 1, 20-28 (1999)
- [3] K. Kobayashi et al., *Journal of Nuclear Science and Technology*, 36, 6, 549-551 (1999)
- [4] T. Oishi et al., *Journal of Radiation Protection Bulletin* (to be published)
- [5] T. Granier et al., *Nucl. Instr. and Meth. in Phys. Res. A* 506, 149-159 (2003)
- [6] K. Kobayashi et al., *Nucl. Instr. and Meth. in Phys. Res. A* 385, 145-156 (1997)
- [7] A. Yamanaka et al., *Journal of Nuclear Science and Technology*, 30, 9, 863-869 (1993)
- [8] S. Yamamoto et al., *Nucl. Sci. Eng.*, 126, 201-212 (1997)
- [9] Y. Ikeuchi, *Proceedings of the 34th symposium at KURRI*, 30 (Japanese)
- [10] D. Rochman et al., *Nucl. Instr. and Meth. in Phys. Res. A* 550 (2005) 397-413

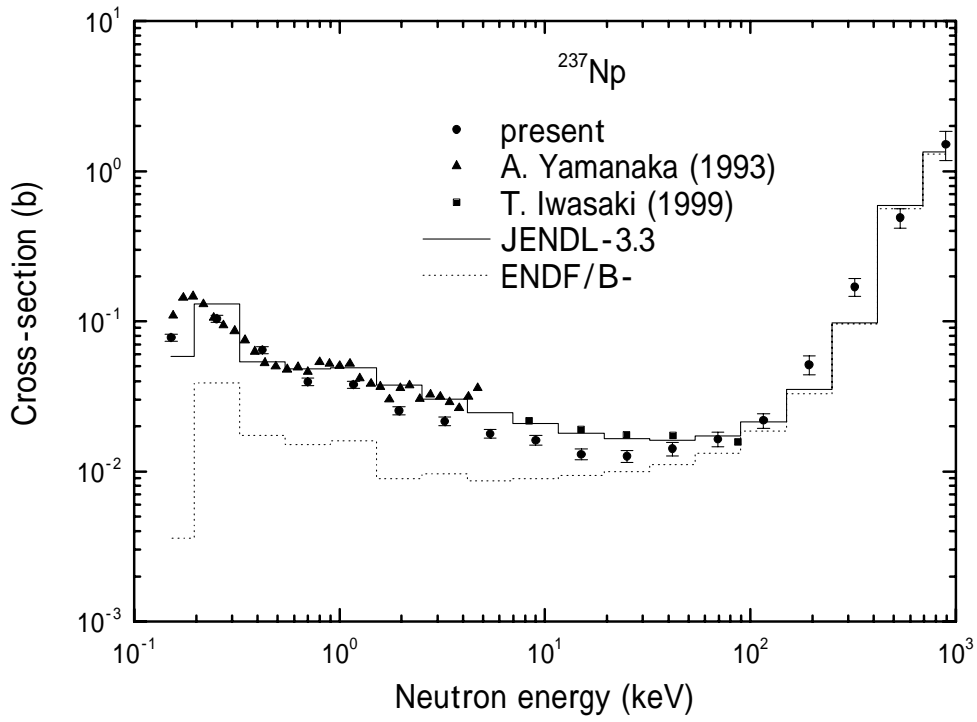


Fig.4 Neutron induced fission cross-section of ^{237}Np

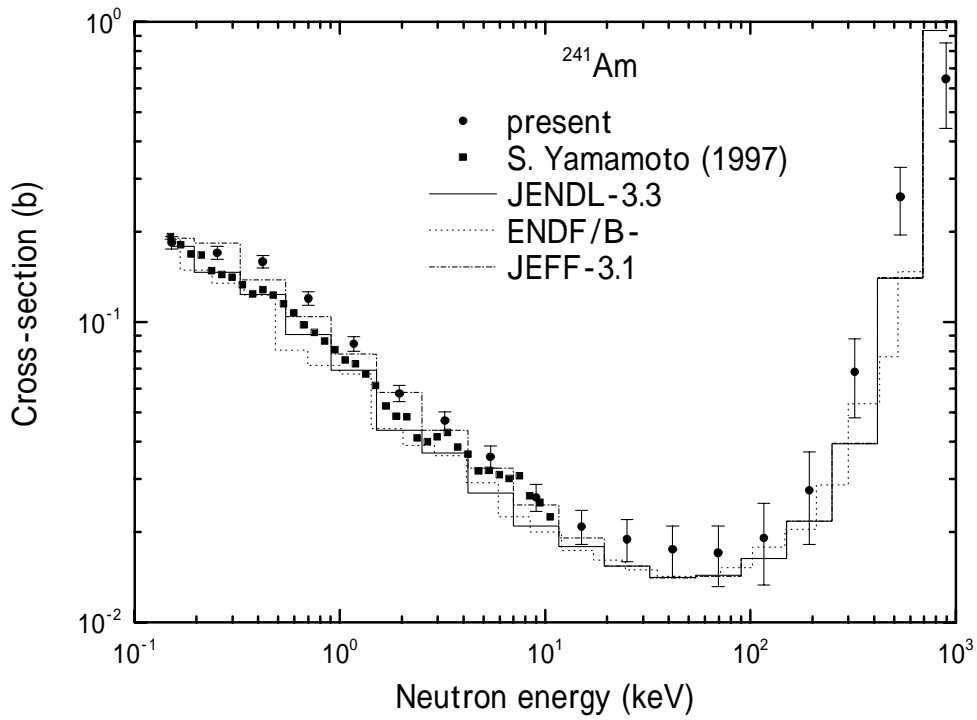


Fig.5 Neutron induced fission cross-section of ^{241}Am